Effects of a reverse shock wave on neutrino oscillations in a new supernova model [*]

Jing Xu(徐晶)[1;1)]   Ming Lu(鲁明)[1;2)]   Xin-Heng Guo(郭新恒)[2;3)]   Li-Jun Hu(胡立军)[3;4)]

[1] Physics Department, Yantai University, Yantai 264005, China
[2] College of Nuclear Science and Techonology, Beijing Normal University, Beijing 100875, China
[3] College of Mechanical and Electrical Engineering, Cangzhou Normal University, Cangzhou 061000, China

Abstract: It is known that in supernova explosions, there might be a reverse shock wave in addition to the forward shock wave during the explosion phase, when the mass of supernova is in a certain range. In this paper, we propose to add the reverse shock wave to the previous supernova model, in which only the forward shock wave was included, and thus obtain a new model. By analyzing the resonance condition as well as the density jump in the new model and using the Landau-Zener method, an expression for the crossing probability in high density matter (P_H) is given. We proceed to study how P_H varies with time and with neutrino energy when both the reverse shock wave and the forward shock wave are considered. From comparison with the previous results, where only the effects of the forward shock wave were considered, it is clear that the reverse shock wave brings significant changes to P_H.

Keywords: neutrino oscillations, shock wave effects, crossing probability, supernova models

PACS: 14.60.Pq, 13.15.+g, 25.30.Pt   **DOI:** 10.1088/1674-1137/42/11/113103

1   Introduction

Since they were first proposed, the effects of supernova (SN) shock waves have been discussed in detail over the past couple of decades [1–6]. A shock wave stems from the sudden change of density profile caused by energy propagating outwards in the process of the explosion. Once the shock wave appears, the density in the SN might undergo abrupt changes, which consequently has a considerable influence on neutrino oscillations. Moreover, it is generally known that neutrino oscillations yield to the distribution of matter density [7–9]. The adiabatic or partially adiabatic neutrino flavor conversion in media with locality or time varying matter density is called the Mikheyev-Smirnov-Wolfenstein (MSW) effect [10–12]. During the supernova explosion, taking into consideration the shock wave effects and MSW effects, the crossing probability of neutrinos in high density matter, P_H, can be obtained by using the Landau-Zener method [13–15].

Supernova neutrino oscillations are also subject to collective effects and Earth matter effects. In Ref. [16], the authors calculated realistic Earth matter effects in the detection of type II SN neutrinos at the Daya Bay reactor neutrino experiment and proposed a possible method to acquire information about the mixing angle, θ_{13}, which was supposed to be smaller than $1.5°$. In Ref. [5], the shock wave effects, MSW effects, collective effects and Earth matter effects in the detection of type II SN neutrinos on the Earth were studied. It was found that the numbers of SN neutrino events depend on the neutrino mass hierarchy, θ_{13} and neutrino masses. In this study, the supernova model in which only the forward shock wave appears during the explosion was applied, and θ_{13} was still assumed to be very small.

In 2012 the Daya Bay Collaboration published the result $\theta_{13} \approx 8.8° \pm 0.8°$ [17], which was different from the previous theoretical predictions. Afterwards, using the θ_{13} value provided by the Daya Bay Collaboration, we calculated the numbers of SN neutrino events from the general supernova model, which is as same as the model in Ref. [5]. It was found that the numbers of neutrino events detected on the Earth depend not only on the mass hierarchy, the average energy of the neutrinos and other inherent parameters, but also rely on the ratio of neutrino luminosity [6]. Finally, we gave the ranges of

SN neutrino event numbers that could be detected at the Daya Bay experiment. Much later, it was found that in some supernovae, when their masses are in a certain range there should be a reverse shock wave which also has a significant impact on neutrino oscillations [18–23]. Therefore, we used the new density data profile from simulations to calculate the survival probability of electron neutrinos and the conversion probability of non-electron neutrinos, and studied matter effects on neutrino oscillations in three different supernova models. Through these results, we could estimate the number of electron neutrinos (and non-electron neutrinos) which remain after they go through the matter in the supernova [24].

In this paper, we will establish a new model for the SN density profile when both the forward shock wave and the reverse shock wave are taken into account. Then in this new model we will give the expression for the crossing probability of neutrinos in high density matter, P_H, and its numerical results. In Section 2, on the basis of the previous supernova model and through data fitting, the new model which contains the forward and reverse shock waves will be established, and the density profile will be obtained. In Section 3, we will analyze where the resonance points occur, taking the density jump into account at the same time, and give the expression for P_H in the new model. How P_H changes as a function of neutrino energy at different times after the supernova explosion will then be plotted. A comparison between the results of the new model and those of the previous model will be given to better reflect the influence of the reverse shock wave. Furthermore, how P_H changes with time when neutrinos take different energy values will be presented. In Section 4, we will summarize the results and give a conclusion.

2   Shock wave models

In our previous work, we used a simple supernova model to study the neutrino oscillations and to calculate numbers of neutrino events detected on the Earth for small and big θ_{13} [5, 6, 16]. For convenience, in this paper this simple model is named Model I, in which the forward shock wave begins one second after the supernova explosion and then spreads outward with time. Now, it is known that the reverse shock wave might be generated posterior to the forward shock wave in some supernova models when the mass of the supernova is in the middle range [24].

In this section, we give a new model containing both the forward shock wave and the reverse shock wave through data fitting. The new model is called Model II for short. For ease of comparison between the final results of the two models, we make the density profile in Model II consistent with that in Model I before the

reverse shock wave occurs. At the same time, we assume that the behavior of the forward shock wave over time basically remains the same in both models. This makes it easy to obtain the function of density distribution in Model II, and to extract the effects of the reverse shock wave on neutrino oscillations from the results in the next section.

As mentioned before, the forward shock wave occurs about 1 s after the explosion. By analyzing the simulated data, however, it is found that the reverse shock wave is stimulated about 2.5 s after the explosion. Both of the shock waves move forward with the arrow of time. When $t < 2.5$ s, the function of the density profile in Model I can still be applied in Model II. However, when $t \geqslant 2.5$ s, some corrections should be made to coincide with the appearance of the reverse shock wave, and then the density profile in Model II can be obtained.

In Model I, due to the forward shock wave the density profile is divided into two cases (0 s $\leqslant t < 1$ s and $t \geqslant 1$ s). The detailed analysis can be found in Ref. [5]. In Model II, because of the forward shock wave and the reverse shock wave, both of them appearing at different times during the period of the explosion, the density profile can be distributed into three situations, i.e. 0 s $\leqslant t < 1$ s, 1 s $\leqslant t < 2.5$ s and $t \geqslant 2.5$ s.

Before the supernova explosion, which is certainly before the appearance of the forward shock wave, the relation between the density profile and the supernova radius is expressed as [25]

$$\rho = \rho_0(r) \simeq 10^{14} \cdot \left(\frac{r}{1 \text{ km}}\right)^{-2.4} \text{ g/cm}^3. \qquad (1)$$

In other words, for 0 s $\leqslant t < 1$ s, Eq. (1) applies in both models.

Then the density curve is divided into two segments at the frontier of the forward shock wave. In Model I, we defined r_s as the frontier of the forward shock wave. In Model II we name it r_{s2} in order to distinguish it from the frontier of the reverse shock wave, which will be called r_{s1} in the following. Accordingly, in Model I for $t \geqslant 1$ s and in Model II for 1 s $\leqslant t < 2.5$ s, the density profile is:

$$\rho(r,t) = \rho_0(r) \cdot \begin{cases} \xi \cdot f(r,t) & (r \leqslant r_{s2}), \\ 1 & (r > r_{s2}). \end{cases} \qquad (2)$$

Here, ξ is the ratio of the potential energies at the two sides of the shock wave frontier, and $f(r,t)$ can be determined by the position of the shock wave frontier. Their expressions were both elaborated in detail in the previous work [5].

For $t \geqslant 2.5$ s, the density curve in Model II is broken into three parts resulting from the forward shock wave and the reverse shock wave. In addition, both of the shock waves move forward with time once generated. The frontier of the forward shock wave, r_{s2}, can be ob-

tained by the expression:

$$r_{s2}(t) = -4.6 \times 10^3 + 1.13 \times 10^4 \cdot t + 1 \times 10^2 \cdot t^2. \qquad (3)$$

Through data fitting, the relation between r_{s2} and r_{s1} is finally obtained. Then the position of the reverse shock frontier can be calculated by

$$\log(r_{s1}(t)) = \log(r_{s2}(t)) - 0.8. \qquad (4)$$

According to the definition of $f(r,t)$ in Ref. [5], at $r = r_{s1}$, it can be deduced that

$$f_{s1}(r,t) = \exp\{[0.28 - 0.69\ln(r_{s2}/\mathrm{km})]$$
$$\times [\arcsin(1 - r_{s1}/r_{s2})]^{1.1}\}. \qquad (5)$$

Using Eq. (2), the density at the frontier of the reverse shock wave, referred to as ρ_{s1}, is

$$\rho_{s1} = 10^{15} \cdot r_{s1}^{-2.4} \cdot f_{s1}(r,t). \qquad (6)$$

Through further data fitting, it is found that the minimum density at the vertical position of the reverse shock wave, defined as $\rho_{1\min}$, has a correlation with ρ_{s1},

$$\log(\rho_{1\min}) = \log(\rho_{s1}) - 0.6. \qquad (7)$$

From the analysis, it can be seen that the first section of the density curve in Model II passes through the point $(r_{s1}, \rho_{1\min})$ in the coordinate system consisting of radius and density. Moreover, it is assumed that in the area where both shock waves have passed over, the density profile of the supernova will basically recover the original distribution. In Model II, for $r < r_{s1}$, the expression of the density profile is nearly the same as Eq. (1), with only the coefficients being slightly different. Between the two shock waves and ahead of the forward shock wave, the density profile is based on and aligned with Eq. (2).
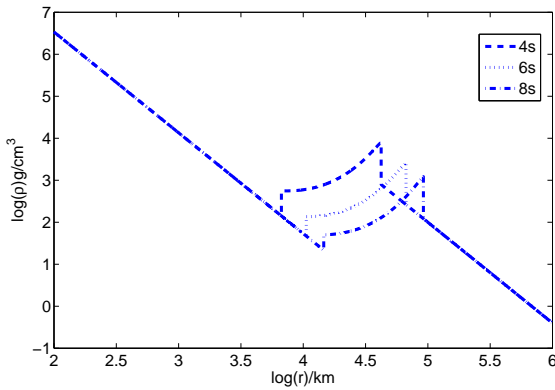

Fig. 1. (color online) Density profiles in Model II at $t = 4, 6, 8$ s.

From the above discussion, we ultimately obtain the expression for the density profile in Model II for $t \geqslant 2.5$ s, as written in Eq. (8). The density profiles as a function

of the supernova radius at three different times after the supernova explosion are plotted in Fig. 1.

$$\rho(r,t) = \begin{cases} 10^{11.33} \cdot r^{-2.4} & (r < r_{s1}), \\ \rho_0(r) \cdot \xi \cdot f(r,t) & (r_{s1} \leqslant r \leqslant r_{s2}), \\ \rho_0(r) & (r > r_{s2}). \end{cases} \qquad (8)$$

3   Calculations of the crossing probability P_H in Model II

In order to calculate the crossing probability in high density matter, P_H, the density jump points and possible resonance points should be analyzed in detail.

In Refs. [10–12], the MSW effects were interpreted as the adiabatic or partially adiabatic neutrino flavor conversion in media with varying matter density. It was found that in a high density medium a flavor is also a mass state propagating without flavor oscillation, unless passing through a resonance where there is a finite probability for flavor change; that is, neutrinos jump from one mass eigenstate to another. Inside the SN, at the high resonance layer ($r = r_i$), the crossing probability P_{Hi} can be obtained using the Landau-Zener formula [13–15]

$$P_{Hi} = \exp\left(-\frac{\pi}{2}\gamma\right), \qquad (9)$$

with

$$\gamma = \frac{|\Delta m_{31}^2|}{2E} \frac{\sin^2 2\theta_{13}}{\cos 2\theta_{13}} \frac{1}{|\mathrm{dln}N_e/\mathrm{d}r|_{\mathrm{res}}}, \qquad (10)$$

where N_e is the electron density and $|\Delta m_{31}^2| \simeq |\Delta m_{32}^2| \simeq 2.4 \times 10^{-3} \mathrm{eV}^2$ [7, 8, 26], and $\theta_{13} = 8.8°$ [17]. At the low resonance region inside the SN the crossing probability P_L can be calculated in the same way, and it is found to be very small. Therefore, in this paper, we ignore P_L.

In the presence of the forward shock wave and the reverse shock wave, P_H cannot be calculated directly, because both shock waves modify the density profiles as shown in the preceding subsection. Within the shock waves and near their frontiers, the matter density is no longer monotonically changing but has a sudden jump, where there might be a resonance point that can satisfy the resonance condition, written as

$$\Delta m_{31}^2 \cdot \cos 2\theta_{13} = 2\sqrt{2} G_F N_e(r_i) E, \qquad (11)$$

with the number density of electrons

$$N_e(r) = N_A \rho(r) Y_e, \qquad (12)$$

where G_F is the Fermi constant, E is the neutrino energy, N_A is Avogadro's constant, and Y_e is the electron fraction, which has a value of 0.5 [5].

For convenience of discussion, the definitions of special positions are given first. The minimum density at the vertical position of the reverse shock wave, as stated in Section 2, is defined as $\rho_{1\min}$. The density at the frontier

of the reverse shock wave is denoted by ρ_{s1}, and similarly ρ_{s2} is the density at the frontier of the forward shock wave. In Model II, the density profile can be viewed as a piecewise function made of three parts. The first part and the third part are oblique lines. The middle section can be considered as a part of a parabolic curve, and at its bottom the minimum density is defined as ρ_{b}. At the top of the parabolic curve, the highest density is defined as $\rho_{2\max}$. ρ_{res} is the resonance density satisfying Eq. (11). From data analysis, some basic relationships of the above density points are revealed as: $\rho_{1\min} < \rho_{b}$, $\rho_{1\min} < \rho_{s2}$, $\rho_{s1} \geqslant \rho_{b}$, $\rho_{s2} < \rho_{2\max}$.

As mentioned earlier, the density curve shown in Fig. 1 consists of three parts, containing two segments of oblique line behind and ahead of the shock waves and a part of a parabolic curve in the middle. The oblique lines of the first and third parts might each have one resonance point, named r_1 and r_3 respectively. On the parabolic curve of the second part, there might be at most two resonance points, r_{21} and r_{22}, lying on the two sides of the minimum density point, respectively. Therefore, there are at most four possible resonance points on the density curve. At the possible resonance points, r_1, r_{21}, r_{22} and r_3, the crossing probability can be expressed in terms of $P_{Hi}(i=1,21,22,3)$.

In addition, the density profile has a sudden change at the frontiers of the reverse shock wave and the forward shock wave, where the crossing probabilities are defined as P_{s1} and P_{s2}, respectively, which are determined by the conservation of flavor across the matter potential discontinuity. They are parts of the whole P_H in Model II. For the derivation of P_{s1} (or P_{s2}), we refer the reader to Refs. [7, 8].

In Model II when $t \geqslant 2.5$ s, it can be shown that there are various situations in which the resonance points might happen as follows:

1) For $\rho_{res} < \rho_{1\min}$ the resonance condition occurs at only one point, $r=r_3$, and then $P_{H1}=P_{H21}=P_{H22}=0$.

2) For $\rho_{res} > \rho_{2\max}$ or $\rho_{s2} < \rho_{res} < \rho_{b}$, the resonance condition occurs at only one point, $r=r_1$, and then $P_{H21}=P_{H22}=P_{H3}=0$.

3) For $\rho_{s2} < \rho_{b}$ and $\rho_{1\min} \leqslant \rho_{res} \leqslant \rho_{s2}$, or $\rho_{s2} = \rho_{b}$ and $\rho_{1\min} \leqslant \rho_{res} < \rho_{s2}$, or $\rho_{s2} > \rho_{b}$ and $\rho_{1\min} \leqslant \rho_{res} < \rho_{b}$, the resonance condition occurs at two points, $r=r_1$ and $r=r_3$, and then $P_{H21}=P_{H22}=0$.

4) When $\rho_{s1} = \rho_{b}$, for $\rho_{s2} < \rho_{s1}$ and $\rho_{s1} \leqslant \rho_{res} \leqslant \rho_{2\max}$, or $\rho_{s2} \geqslant \rho_{s1}$ and $\rho_{s2} < \rho_{res} \leqslant \rho_{2\max}$; and when $\rho_{s1} > \rho_{b}$, for $\rho_{s2} \leqslant \rho_{s1}$ and $\rho_{s1} < \rho_{res} \leqslant \rho_{2\max}$, or $\rho_{s2} > \rho_{s1}$ and $\rho_{s2} < \rho_{res} \leqslant \rho_{2\max}$, the resonance condition occurs at two points, $r=r_1$ and $r=r_{22}$, and then $P_{H21}=P_{H3}=0$.

5) For $\rho_{s2} < \rho_{b}$ and $\rho_{res} = \rho_{b}$, the resonance condition occurs at two points, $r=r_1$ and $r=r_{21}$ (the two points r_{21} and r_{22} concide), and then $P_{H22}=P_{H3}=0$.

6) When $\rho_{s1} = \rho_{b}$, for $\rho_{s2} > \rho_{s1}$ and $\rho_{s1} \leqslant \rho_{res} \leqslant \rho_{s2}$; and when $\rho_{s1} > \rho_{b}$, for $\rho_{s2} > \rho_{s1}$ and $\rho_{s1} < \rho_{res} \leqslant \rho_{s2}$, the resonance condition occurs at three points, $r=r_1$, $r=r_{22}$ and $r=r_3$, and then $P_{H21}=0$.

7) For $\rho_{s2} \geqslant \rho_{b}$ and $\rho_{res} = \rho_{b}$, the resonance condition occurs at three points, $r=r_1$, $r=r_{21}$ and $r=r_3$ (the two points r_{21} and r_{22} coincide), and then $P_{H22}=0$.

8) When $\rho_{s1} > \rho_{b}$, for $\rho_{s2} \leqslant \rho_{b}$ and $\rho_{b} < \rho_{res} \leqslant \rho_{s1}$, or $\rho_{b} < \rho_{s2} < \rho_{s1}$ and $\rho_{s2} < \rho_{res} \leqslant \rho_{s1}$, the resonance condition occurs at three points, $r=r_1$, $r=r_{21}$ and $r=r_{22}$, and then $P_{H3}=0$.

9) When $\rho_{s1} > \rho_{b}$, for $\rho_{b} < \rho_{s2} \leqslant \rho_{s1}$ and $\rho_{b} < \rho_{res} < \rho_{s2}$, or $\rho_{s2} > \rho_{s1}$ and $\rho_{b} < \rho_{res} \leqslant \rho_{s1}$, the resonance condition occurs at four points, $r=r_1$, $r=r_{21}$, $r=r_{22}$, and $r=r_3$.

Taking all the above situations into account, for $t \geqslant 2.5$ s in Model II the expression for P_H can be obtained as follows:

$$
\begin{aligned}
P_H = {}& (P_{H1}+P_{s1}+P_{H21}+P_{H22}+P_{s2}+P_{H3}) \\
& -2(P_{H1}P_{s1}+P_{H1}P_{H21}+P_{H1}P_{H22}+P_{H1}P_{s2}+P_{H1}P_{H3} \\
& +P_{s1}P_{H21}+P_{s1}P_{H22}+P_{s1}P_{s2}+P_{s2}P_{H3}+P_{H21}P_{H22} \\
& +P_{H21}P_{s2}+P_{H21}P_{H3}+P_{H22}P_{s2}+P_{H22}P_{H3}+P_{s2}P_{H3}) \\
& +4(P_{H1}P_{s1}P_{H21}+P_{H1}P_{s1}P_{H22}+P_{H1}P_{s1}P_{s2}+P_{H1}P_{s1}P_{H3}+P_{H1}P_{H21}P_{H22} \\
& +P_{H1}P_{H21}P_{s2}+P_{H1}P_{H21}P_{H3}+P_{H1}P_{H22}P_{s2}+P_{H1}P_{H22}P_{H3}+P_{H1}P_{s2}P_{H3} \\
& +P_{s1}P_{H21}P_{H22}+P_{s1}P_{H21}P_{s2}+P_{s1}P_{H21}P_{H3}+P_{s1}P_{H22}P_{s2}+P_{s1}P_{H22}P_{H3} \\
& +P_{s1}P_{s2}P_{H3}+P_{H21}P_{H22}P_{s2}+P_{H21}P_{H22}P_{H3}+P_{H21}P_{s2}P_{H3}+P_{H22}P_{s2}P_{H3}) \\
& -8(P_{H1}P_{s1}P_{H21}P_{H22}+P_{H1}P_{s1}P_{H21}P_{s2}+P_{H1}P_{s1}P_{H21}P_{H3} \\
& +P_{H1}P_{s1}P_{H22}P_{s2}+P_{H1}P_{s1}P_{H22}P_{H3}+P_{H1}P_{s1}P_{s2}P_{H3}+P_{H1}P_{H21}P_{H22}P_{s2} \\
& +P_{H1}P_{H21}P_{H22}P_{H3}+P_{H1}P_{H21}P_{s2}P_{H3}+P_{H1}P_{H22}P_{s2}P_{H3}+P_{s1}P_{H21}P_{H22}P_{s2} \\
& +P_{s1}P_{H21}P_{H22}P_{H3}+P_{s1}P_{H21}P_{s2}P_{H3}+P_{s1}P_{H22}P_{s2}P_{H3}+P_{H21}P_{H22}P_{s2}P_{H3}) \\
& +16(P_{H1}P_{s1}P_{H21}P_{H22}P_{s2}+P_{H1}P_{s1}P_{H21}P_{H22}P_{H3}+P_{H1}P_{s1}P_{H21}P_{s2}P_{H3} \\
& +P_{H1}P_{s1}P_{H22}P_{s2}P_{H3}+P_{H1}P_{H21}P_{H22}P_{s2}P_{H3}+P_{s1}P_{H21}P_{H22}P_{s2}P_{H3})
\end{aligned}
$$

$-32P_{H1}P_{s1}P_{H21}P_{H22}P_{s2}P_{H3}$

$+2\{[1-2(P_{H21}+P_{H22}+P_{s2}+P_{H3})$

$+4(P_{H21}P_{H22}+P_{H21}P_{s2}+P_{H21}P_{H3}+P_{H22}P_{s2}+P_{H22}P_{H3}+P_{s2}P_{H3})$

$-8(P_{H21}P_{H22}P_{s2}+P_{H21}P_{H22}P_{H3}+P_{H21}P_{s2}P_{H3}+P_{H22}P_{s2}P_{H3})$

$+16P_{H21}P_{H22}P_{s2}P_{H3}]\sqrt{P_{H1}P_{s1}(1-P_{H1})(1-P_{s1})}\cos\phi_{1s1}$

$+[1-2(P_{s1}+P_{H22}+P_{s2}+P_{H3})$

$+4(P_{s1}P_{H22}+P_{s1}P_{s2}+P_{s1}P_{H3}+P_{H22}P_{s2}+P_{H22}P_{H3}+P_{s2}P_{H3})$

$-8(P_{s1}P_{H22}P_{s2}+P_{s1}P_{H22}P_{H3}+P_{s1}P_{s2}P_{H3}+P_{H22}P_{s2}P_{H3})$

$+16P_{s1}P_{H22}P_{s2}P_{H3}]\sqrt{P_{H1}P_{H21}(1-P_{H1})(1-P_{H21})}\cos(\phi_{1s1}+\phi_{s121})$

$+[1-2(P_{s1}+P_{H21}+P_{s2}+P_{H3})$

$+4(P_{s1}P_{H21}+P_{s1}P_{s2}+P_{s1}P_{H3}+P_{H21}P_{s2}+P_{H21}P_{H3}+P_{s2}P_{H3})$

$-8(P_{s1}P_{H21}P_{s2}+P_{s1}P_{H21}P_{H3}+P_{s1}P_{s2}P_{H3}+P_{H21}P_{s2}P_{H3})$

$+16P_{s1}P_{H21}P_{s2}P_{H3}]\sqrt{P_{H1}P_{H22}(1-P_{H1})(1-P_{H22})}\cos(\phi_{1s1}+\phi_{s121}+\phi_{2122})$

$+[1-2(P_{s1}+P_{H21}+P_{H22}+P_{H3})$

$+4(P_{s1}P_{H21}+P_{s1}P_{H22}+P_{s1}P_{H3}+P_{H21}P_{H22}+P_{H21}P_{H3}+P_{H22}P_{H3})$

$-8(P_{s1}P_{H21}P_{H22}+P_{s1}P_{H21}P_{H3}+P_{s1}P_{H22}P_{H3}+P_{H21}P_{H22}P_{H3})$

$+16P_{s1}P_{H21}P_{H22}P_{H3}]\sqrt{P_{H1}P_{s2}(1-P_{H1})(1-P_{s2})}\cos(\phi_{1s1}+\phi_{s121}+\phi_{2122}+\phi_{22s2})$

$+[1-2(P_{s1}+P_{H21}+P_{H22}+P_{s2})$

$+4(P_{s1}P_{H21}+P_{s1}P_{H22}+P_{s1}P_{s2}+P_{H21}P_{H22}+P_{H21}P_{s2}+P_{H22}P_{s2})$

$-8(P_{s1}P_{H21}P_{H22}+P_{s1}P_{H21}P_{s2}+P_{s1}P_{H22}P_{s2}+P_{H21}P_{H22}P_{s2})$

$+16P_{s1}P_{H21}P_{H22}P_{s2}]\sqrt{P_{H1}P_{H3}(1-P_{H1})(1-P_{H3})}\cos(\phi_{1s1}+\phi_{s121}+\phi_{2122}+\phi_{22s2}+\phi_{s23})$

$+[1-2(P_{H1}+P_{H22}+P_{s2}+P_{H3})$

$+4(P_{H1}P_{H22}+P_{H1}P_{s2}+P_{H1}P_{H3}+P_{H22}P_{s2}+P_{H22}P_{H3}+P_{s2}P_{H3})$

$-8(P_{H1}P_{H22}P_{s2}+P_{H1}P_{H22}P_{H3}+P_{H1}P_{s2}P_{H3}+P_{H22}P_{s2}P_{H3})$

$+16P_{H1}P_{H22}P_{s2}P_{H3}]\sqrt{P_{s1}P_{H21}(1-P_{s1})(1-P_{H21})}\cos\phi_{s121}$

$+[1-2(P_{H1}+P_{H21}+P_{s2}+P_{H3})$

$+4(P_{H1}P_{H21}+P_{H1}P_{s2}+P_{H1}P_{H3}+P_{H21}P_{s2}+P_{H21}P_{H3}+P_{s2}P_{H3})$

$-8(P_{H1}P_{H21}P_{s2}+P_{H1}P_{H21}P_{H3}+P_{H1}P_{s2}P_{H3}+P_{H21}P_{s2}P_{H3})$

$+16P_{H1}P_{H21}P_{s2}P_{H3}]\sqrt{P_{s1}P_{H22}(1-P_{s1})(1-P_{H22})}\cos(\phi_{s121}+\phi_{2122})$

$+[1-2(P_{H1}+P_{H21}+P_{H22}+P_{H3})$

$+4(P_{H1}P_{H21}+P_{H1}P_{H22}+P_{H1}P_{H3}+P_{H21}P_{H22}+P_{H21}P_{H3}+P_{H22}P_{H3})$

$-8(P_{H1}P_{H21}P_{H22}+P_{H1}P_{H21}P_{H3}+P_{H1}P_{H22}P_{H3}+P_{H21}P_{H22}P_{H3})$

$+16P_{H1}P_{H21}P_{H22}P_{H3}]\sqrt{P_{s1}P_{s2}(1-P_{s1})(1-P_{s2})}\cos(\phi_{s121}+\phi_{2122}+\phi_{22s2})$

$+[1-2(P_{H1}+P_{H21}+P_{H22}+P_{s2})$

$+4(P_{H1}P_{H21}+P_{H1}P_{H22}+P_{H1}P_{s2}+P_{H21}P_{H22}+P_{H21}P_{s2}+P_{H22}P_{s2})$

$-8(P_{H1}P_{H21}P_{H22}+P_{H1}P_{H21}P_{s2}+P_{H1}P_{H22}P_{s2}+P_{H21}P_{H22}P_{s2})$

$+16P_{H1}P_{H21}P_{H22}P_{s2}]\sqrt{P_{s1}P_{H3}(1-P_{s1})(1-P_{H3})}\cos(\phi_{s121}+\phi_{2122}+\phi_{22s2}+\phi_{s23})$

$+[1-2(P_{H1}+P_{s1}+P_{s2}+P_{H3})$

$+4(P_{H1}P_{s1}+P_{H1}P_{s2}+P_{H1}P_{H3}+P_{s1}P_{s2}+P_{s1}P_{H3}+P_{s2}P_{H3})$

$-8(P_{H1}P_{s1}P_{s2}+P_{H1}P_{s1}P_{H3}+P_{H1}P_{s2}P_{H3}+P_{s1}P_{s2}P_{H3})$

$+16P_{H1}P_{s1}P_{s2}P_{H3}]\sqrt{P_{H21}P_{H22}(1-P_{H21})(1-P_{H22})}\cos\phi_{2122}$

$+[1-2(P_{H1}+P_{s1}+P_{H22}+P_{H3})$

$+4(P_{H1}P_{s1}+P_{H1}P_{H22}+P_{H1}P_{H3}+P_{s1}P_{H22}+P_{s1}P_{H3}+P_{H22}P_{H3})$

$$-8(P_{H1}P_{s1}P_{H22}+P_{H1}P_{s1}P_{H3}+P_{H1}P_{H22}P_{H3}+P_{s1}P_{H22}P_{H3})$$

$$+16P_{H1}P_{s1}P_{H22}P_{H3}]\sqrt{P_{H21}P_{s2}(1-P_{H21})(1-P_{s2})}\cos(\phi_{2122}+\phi_{22s2})$$

$$+[1-2(P_{H1}+P_{s1}+P_{H22}+P_{s2})$$

$$+4(P_{H1}P_{s1}+P_{H1}P_{H22}+P_{H1}P_{s2}+P_{s1}P_{H22}+P_{s1}P_{s2}+P_{H22}P_{s2})$$

$$-8(P_{H1}P_{s1}P_{H22}+P_{H1}P_{s1}P_{s2}+P_{H1}P_{H22}P_{s2}+P_{s1}P_{H22}P_{s2})$$

$$+16P_{H1}P_{s1}P_{H22}P_{s2}]\sqrt{P_{H21}P_{H3}(1-P_{H21})(1-P_{H3})}\cos(\phi_{2122}+\phi_{22s2}+\phi_{s23})$$

$$+[1-2(P_{H1}+P_{s1}+P_{H21}+P_{H3})$$

$$+4(P_{H1}P_{s1}+P_{H1}P_{H21}+P_{H1}P_{H3}+P_{s1}P_{H21}+P_{s1}P_{H3}+P_{H21}P_{H3})$$

$$-8(P_{H1}P_{s1}P_{H21}+P_{H1}P_{s1}P_{H3}+P_{H1}P_{H21}P_{H3}+P_{s1}P_{H21}P_{H3})$$

$$+16P_{H1}P_{s1}P_{H21}P_{H3}]\sqrt{P_{H22}P_{s2}(1-P_{H22})(1-P_{s2})}\cos(\phi_{22s2})$$

$$+[1-2(P_{H1}+P_{s1}+P_{H21}+P_{s2})$$

$$+4(P_{H1}P_{s1}+P_{H1}P_{H21}+P_{H1}P_{s2}+P_{s1}P_{H21}+P_{s1}P_{s2}+P_{H21}P_{s2})$$

$$-8(P_{H1}P_{s1}P_{H21}+P_{H1}P_{s1}P_{s2}+P_{H1}P_{H21}P_{s2}+P_{s1}P_{H21}P_{s2})$$

$$+16P_{H1}P_{s1}P_{H21}P_{s2}]\sqrt{P_{H22}P_{H3}(1-P_{H22})(1-P_{H3})}\cos(\phi_{22s2}+\phi_{s23})$$

$$+[1-2(P_{H1}+P_{s1}+P_{H21}+P_{H22})$$

$$+4(P_{H1}P_{s1}+P_{H1}P_{H21}+P_{H1}P_{H22}+P_{s1}P_{H21}+P_{s1}P_{H22}+P_{H21}P_{H22})$$

$$-8(P_{H1}P_{s1}P_{H21}+P_{H1}P_{s1}P_{H22}+P_{H1}P_{H21}P_{H22}+P_{s1}P_{H21}P_{H22})$$

$$+16P_{H1}P_{s1}P_{H21}P_{H22}]\sqrt{P_{s2}P_{H3}(1-P_{s2})(1-P_{H3})}\cos\phi_{s23}\}$$

$$-8\{[1-2(P_{H1}+P_{s1})+4P_{H1}P_{s1}]\sqrt{P_{H21}P_{H22}(1-P_{H21})(1-P_{H22})}\cos\phi_{2122}$$

$$\sqrt{P_{s2}P_{H3}(1-P_{s2})(1-P_{H3})}\cos\phi_{s23}$$

$$+[1-2(P_{H1}+P_{H21})+4P_{H1}P_{H21}]\sqrt{P_{s1}P_{H22}(1-P_{s1})(1-P_{H22})}\cos(\phi_{s121}+\phi_{2122})$$

$$\sqrt{P_{s2}P_{H3}(1-P_{s2})(1-P_{H3})}\cos\phi_{s23}$$

$$+[1-2(P_{H1}+P_{H22})+4P_{H1}P_{H22}]\sqrt{P_{s1}P_{H21}(1-P_{s1})(1-P_{H21})}\cos\phi_{s121}$$

$$\sqrt{P_{s2}P_{H3}(1-P_{s2})(1-P_{H3})}\cos\phi_{s23}$$

$$+[1-2(P_{H1}+P_{s2})+4P_{H1}P_{s2}]\sqrt{P_{s1}P_{H21}(1-P_{s1})(1-P_{H21})}\cos\phi_{s121}$$

$$\sqrt{P_{H22}P_{H3}(1-P_{H22})(1-P_{H3})}\cos(\phi_{22s2}+\phi_{s23})$$

$$+[1-2(P_{H1}+P_{H3})+4P_{H1}P_{H3}]\sqrt{P_{s1}P_{H21}(1-P_{s1})(1-P_{H21})}\cos\phi_{s121}$$

$$\sqrt{P_{H22}P_{s2}(1-P_{H22})(1-P_{s2})}\cos\phi_{22s2}$$

$$+[1-2(P_{s1}+P_{H21})+4P_{s1}P_{H21}]\sqrt{P_{H1}P_{H22}(1-P_{H1})(1-P_{H22})}\cos(\phi_{1s1}+\phi_{s121}+\phi_{2122})$$

$$\sqrt{P_{s2}P_{H3}(1-P_{s2})(1-P_{H3})}\cos\phi_{s23}$$

$$+[1-2(P_{s1}+P_{H22})+4P_{s1}P_{H22}]\sqrt{P_{H1}P_{H21}(1-P_{H1})(1-P_{H21})}\cos(\phi_{1s1}+\phi_{s121})$$

$$\sqrt{P_{s2}P_{H3}(1-P_{s2})(1-P_{H3})}\cos\phi_{s23}$$

$$+[1-2(P_{s1}+P_{s2})+4P_{s1}P_{s2}]\sqrt{P_{H1}P_{H21}(1-P_{H1})(1-P_{H21})}\cos(\phi_{1s1}+\phi_{s121})$$

$$\sqrt{P_{H22}P_{H3}(1-P_{H22})(1-P_{H3})}\cos(\phi_{22s2}+\phi_{s23})$$

$$+[1-2(P_{s1}+P_{H3})+4P_{s1}P_{H3}]\sqrt{P_{H1}P_{H21}(1-P_{H1})(1-P_{H21})}\cos(\phi_{1s1}+\phi_{s121})$$

$$\sqrt{P_{H22}P_{s2}(1-P_{H22})(1-P_{s2})}\cos(\phi_{22s2})$$

$$+[1-2(P_{H21}+P_{H22})+4P_{H21}P_{H22}]\sqrt{P_{H1}P_{s1}(1-P_{H1})(1-P_{s1})}\cos\phi_{1s1}$$

$$\sqrt{P_{s2}P_{H3}(1-P_{s2})(1-P_{H3})}\cos\phi_{s23}$$

$$+[1-2(P_{H21}+P_{s2})+4P_{H21}P_{s2}]\sqrt{P_{H1}P_{s1}(1-P_{H1})(1-P_{s1})}\cos\phi_{1s1}$$

$$\sqrt{P_{H22}P_{H3}(1-P_{H22})(1-P_{H3})}\cos(\phi_{22s2}+\phi_{s23})$$

$$+[1-2(P_{H21}+P_{H3})+4P_{H21}P_{H3}]\sqrt{P_{H1}P_{s1}(1-P_{H1})(1-P_{s1})}\cos\phi_{1s1}$$

$$\sqrt{P_{H22}P_{s2}(1-P_{H22})(1-P_{s2})}\cos\phi_{22s2}$$

$$+[1-2(P_{H22}+P_{s2})+4P_{H22}P_{s2}]\sqrt{P_{H1}P_{s1}(1-P_{H1})(1-P_{s1})}\cos\phi_{1s1}$$

$$\sqrt{P_{H21}P_{H3}(1-P_{H21})(1-P_{H3})}\cos(\phi_{2122}+\phi_{22s2}+\phi_{s23})$$

$$+[1-2(P_{H22}+P_{H3})+4P_{H22}P_{H3}]\sqrt{P_{H1}P_{s1}(1-P_{H1})(1-P_{s1})}\cos(\phi_{1s1})$$

$$\sqrt{P_{H21}P_{s2}(1-P_{H21})(1-P_{s2})}\cos(\phi_{2122}+\phi_{22s2})$$

$$+[1-2(P_{s2}+P_{H3})+4P_{s2}P_{H3}]\sqrt{P_{H1}P_{s1}(1-P_{H1})(1-P_{s1})}\cos\phi_{1s1}$$

$$\sqrt{P_{H21}P_{H22}(1-P_{H21})(1-P_{H22})}\cos\phi_{2122}\}$$

$$+32\sqrt{P_{H1}P_{s1}P_{H21}P_{H22}P_{s2}P_{H3}(1-P_{H1})(1-P_{s1})(1-P_{H21})(1-P_{H22})(1-P_{s2})(1-P_{H3})}$$

$$\times\cos\phi_{1s1}\cos\phi_{2122}\cos\phi_{s23}. \tag{13}$$

In the above equation, ϕ_{ij} $(i, j=1, s1, 21, 22, s2, 3)$ is defined in Eq. (14), and its value is different from that in Ref. [5] because here we take $\theta_{13}=8.8°$ as provided by the Daya Bay Collaboration:

$$\phi_{ij} \approx \int_{r_i}^{r_j} \mathrm{d}x \frac{1}{2E}$$
$$\times\sqrt{[\Delta m_{31}^2\cos2\theta_{13}-2EV(r)]^2+(\Delta m_{31}^2\sin2\theta_{13})^2}, \tag{14}$$

where the physical meaning of E and the value of Δm_{31}^2 are the same as in Eq. (11). $V(r)$ is the SN matter potential, which is determined by N_e as follows:

$$V(r)=\sqrt{2}G_F N_e(r), \tag{15}$$

In Fig. 2 we plot P_H as a function of the neutrino energy E, at t = 4 s, 6 s, 8 s in Model II. In order to see the effects of the reverse shock wave on P_H in an explicit way, we also plot the P_H in Model I as a comparison.

In Fig. 2, the curves of P_H in Model II are different from those in Model I, which confirms that the reverse shock wave indeed affects neutrino oscillations. In each of the three figures, the two curves partially overlap at the beginning and the overlapping portion increases with time. This can be interpreted as the appearance of the reverse shock wave not affecting neutrino oscillations at low neutrino energy. However, with increasing neutrino energy, the two curves separate from each other. In other words, the effect of the reverse shock wave on P_H becomes more obvious when the neutrino energy reaches a certain value. In Fig. 2(a) especially, there is a considerable difference between the two curves for $E> 5$ MeV. The curve of Model II has two sharp peaks while the curve of Model I only has one gentle peak. This demonstrates that early in the explosion the reverse shock wave has a great influence on neutrino oscillations, resulting in the complicated variations of P_H. Nevertheless, it is found that this influence gets weaker over time because both of the shock waves constantly move forward with the explosion and will eventually sweep out of the supernova. This can be confirmed by Fig. 2(c), in which there is more overlap between the two curves and their variations gradually tend to converge compared with Fig. 2(a) and Fig. 2(b).
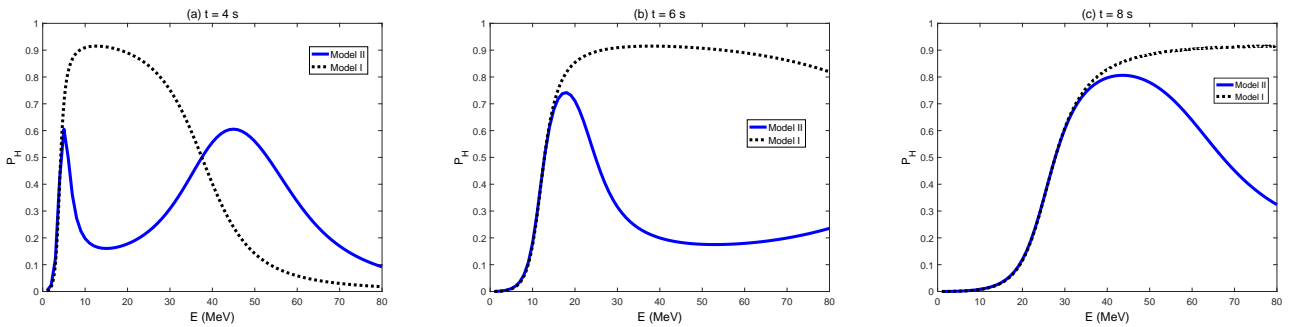

Fig. 2.   (color online) The crossing probability P_H as a function of the neutrino energy E at three different times t = 4 s, 6 s, 8 s.
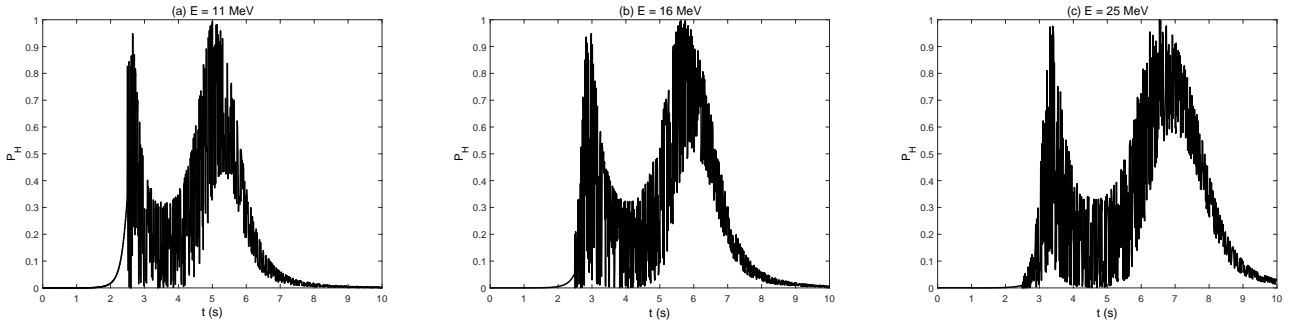
Fig. 3.   The crossing probability P_H as a function of time t for three different neutrino energies in Model II.

In Fig. 3, we plot P_H as a function of time for three different values of E: 11, 16 and 25 MeV, respectively. It can be seen that in the three figures the oscillating curves have two peaks in the vibration process of P_H. Furthermore, the interval between the two peaks enlarges, and both of the peaks move to higher t as E increases. Moreover, P_H oscillates more frequently as the neutrino energy goes up. The variation of P_H is very different from that in Ref. [5], because the value of θ_{13} and the reverse shock wave both have important effects on neutrino oscillations.

In order to see the impact of the reverse shock wave on neutrino oscillations directly, we further estimate the numbers of supernova neutrino events detected on the Earth. Here we choose the neutrino-carbon reaction channel in the Daya Bay experiment as an example in which all flavors of neutrinos are involved. It is assumed that all supernova neutrinos come from a "standard" supernova. All the parameters, including those associated with the "standard" supernova, supernova neutrinos and the reaction cross section can be found in Ref. [6]. We find that in the case of normal(inverted) mass hierarchy, the number of events varies between 78 and 150 in the ranges of the model parameters when the reverse shock wave effects are taken into account. When there is no reverse shock wave, the number of events changes between 50 and 95.

4   Discussion and summary

In this paper, on the basis of simulation data, a new supernova model has been proposed which contains both the reverse shock wave and the forward shock wave. The function for the density profile changing with time in the new model was proposed through data fitting. It was found that the reverse shock wave begins at $t=2.5$ s posterior to the forward shock wave, which starts at $t=1$ s after the supernova explosion. The same as the forward shock wave, the reverse shock wave also moves forward over time. We analyzed all possible situations of the density resonance points, combining with the density jump and using the Landau-Zener method, then gave the expression for P_H in the new model. Moreover, we calculated and plotted the variations of P_H with the neutrino energy for three different times after the supernova explosion and made a comparison with the results of the previous model. It was confirmed that the reverse shock wave had a significant impact on neutrino oscillations. Finally, we plotted P_H as a function of time for three fixed values of E. The changing behavior of P_H is strongly dependent on E. In addition, by comparing the numbers of neutrino events in the two models, it is discovered that the reverse shock wave can increase the number of events detected on the Earth in the neutrino-carbon channel.

It still requires a lot of effort to identify the SN models and the four physical effects including the shock wave effects, MSW effects, collective effects and Earth matter effects. At present, our research on the collective effects and supernova simulations is still in progress. In the near future, considering all of the physical effects on supernova neutrino oscillations and applying the updated simulation results for supernova models, it should be possible to get more accurate predictions of the numbers of supernova neutrinos detected on the Earth.

References

1 G. L. Fogli, E. Lisi, D. Montanino, and A. Mirizzi, Phys. Rev. D, **68**: 033005 (2003), [hep-ph/0304056]
2 G. L. Fogli, E. Lisi, A. Mirizzi, and D. Montanino, JCAP, **04**: 002 (2005), [hep-ph/0412046]
3 G. L. Fogli, E. Lisi, A. Mirizzi, and D. Montanino, JCAP, **06**: 012 (2006), [hep-ph/0603033]
4 R. C. Schirato and G. M. Fuller, [hep-ph/0205390]
5 M. Y. Huang, X. H. Guo, and B. L. Young, Phys. Rev. D, **82**: 033011 (2010), arXiv:1003.1197 [astro-ph.HE]
6 J. Xu, M. Y. Huang, L. J. Hu, X. H. Guo, and B. L. Young,

Commun. Theor. Phys., **61**(2): 2, 226 (2014)

7 T. K. Kuo and J. T. Pantaleone, Rev. Mod. Phys., **61**: 937 (1989)

8 T. K. Kuo and J. T. Pantaleone, Phys. Rev. D, **39**: 1930 (1989)

9 K. Kotake, K. Sato, and K. Takahashi, Rept. Prog. Phys., **69**: 971 (2006)

10 S. P. Mikheev and A. Y. Smirnov, Sov. J. Nucl. Phys., **42**: 913 (1985), [Yad. Fiz., **42**: 1441 (1985)]

11 S. P. Mikheev and A. Y. Smirnov, Sov. Phys. JETP, **64**: 4 (1986), arXiv:0706.0454 [hep-ph]

12 L. Wolfenstein, Phys. Rev. D, **17**: 2369 (1978)

13 Landau. L., Phys. Z. Sowjetunion, **2**: 46 (1932).

14 C. Zener, Proc. R. Soc. A, **137**: 696 (1932)

15 L. D. Landau and E. M. Lifshitz, Quantum Mechanics: Non-Relativistic Theory (Pergamon, New York) 1977.

16 X. H. Guo, M. Y. Huang, and B. L. Young, Phys. Rev. D, **79**: 113007 (2009), arXiv:0806.2720 [hep-ph]

17 F. P. An et al (DAYA-BAY Collaboration), Phys. Rev. Lett., **108**: 171803 (2012), arXiv:1203.1669 [hep-ex]

18 J. Kneller, C. Volpe, Phys. Rev. D, **82**: 123004 (2010), arXiv:1006.0913[astro-ph.HE]

19 T. Lund and J. P. Kneller, Phys. Rev. D, **88**: 02308 (2013), arXiv:1304.6372 [hep-ph]

20 S. Galais, J. Kneller, C. Volpe, and J. Gava, Phys. Rev. D, **81**: 053002 (2010), arXiv:0906.5294 [hep-ph]

21 K. M. Patton, J. P. Kneller, and G. C. McLaughlin, Phys. Rev. D, **89**: 073022 (2014), arXiv:1310.5643 [hep-ph]

22 A. Wongwathanarat, E. Mueller, and H. T. Janka, Astron. Astrophys., **577**: A48 (2015), arXiv:1409.5431 [astro-ph.HE]

23 S. M. Couch and C. D. Ott, arXiv:1408.1399 [astro-ph.HE]

24 J. Xu, L. J. Hu, R. C. Li, X. H. Guo, and B. L. Young, Commun. Theor. Phys., **65**(4): 506 (2016)

25 H. A. Bethe, Rev. Mod. Phys., **62**: 801 (1990); G. E. Brown, H. A. Bethe, and G. Baym, Nucl. Phys. A, **375**: 481 (1982)

26 M. C. Gonzalez-Garcia and M. Maltoni, Phys. Rep., **460**: 1 (2008); T. Schwetz, M. Tortola, and J. W. F. Valle, New. J. Phys., **10**: 113011 (2008)